Circ_DLG1 facilitates esophageal squamous cell carcinoma progression by mediating miR-338-3p/MAP3K9 axis via activating MAPK/ERK pathway

Yixuan Yang
the First Affiliated Hospital of Xiamen
Bing Zhu
Hubei Provincial Hospital of Integrated Chinese and Western Medicine
Zhaofeng Ning
Tai'an Tumor Hospital
Xiaodong Wang
Air Force Hospital in Western War Zone
Zhaoxia Li
PLA Rocket Force Characteristic Medical Center
Chunxia Zhang
Inner Mongolia Forestry General Hospital
Linchun Wen (u9d2xq@163.com)
Suqian Hospital Affiliated to Xuzhou Medical University

Research

Keywords: circ_DLG1, miR-338-3p, MAP3K9, ESCC, MAPK/ERK

Posted Date: March 10th, 2020

DOI: https://doi.org/10.21203/rs.3.rs-16608/v1

Abstract

Background: Esophageal squamous cell carcinoma (ESCC) is an aggressive malignancy with a high incidence and poor prognosis. The document of circular RNAs (circRNAs) is frequently associated with cancer development. This study intended to explore the functional mechanism of circ_DLG1 in ESCC.

Methods: The expression of circ_DLG1, miR-338-3p and Mitogen-Activated Protein Kinase Kinase Kinase 9 (MAP3K9) was measured by quantitative real-time polymerase chain reaction (qRT-PCR). Cell cycle, proliferation, migration and invasion were performed for functional analysis using flow cytometry, 3-(4, 5-dimethylthiazol-2-yl)-2, 5-diphenyltetrazolium bromide (MTT) and transwell assay, respectively. The protein levels of MAP3K9, p38, phosphor p38 (p-p38), ERK1/2, phosphor ERK1/2 (p-ERK1/2) were detected by western blot. Bioinformatics tool for target prediction used the online tool starBase. Dual-luciferase reporter assay was performed to verify the target relationship. The animal experiments were performed to ascertain the role of circ_DLG1 *in vivo*.

Results: The expression of circ_DLG1 was elevated in ESCC tissues, plasma and cells. Circ_DLG1 knockdown inhibited cell cycle, proliferation, migration and invasion. MAP3K9 was highly expressed in ESCC tissues and cells, and its overexpression rescued the effects of circ_DLG1 knockdown. MiR-338-3p was a link between circ_DLG1 and MAP3K9, and circ_DLG1 regulated the expression of MAP3K9 by targeting miR-338-3p. The MAPK/ERK pathway was involved in the circ_DLG1/miR-338-3p/MAP3K9 regulatory axis. Circ_DLG1 knockdown blocked the tumor growth *in vivo* by regulating miR-338-3p and MAP3K9.

Conclusion: Circ_DLG1 contributed to the malignant progression of ESCC by mediating the miR-338-3p/MAP3K9 axis via activating the MAPK/ERK signaling pathway. This paper provided a novel action mode of circ_DLG1 in ESCC.

Background

Esophageal cancer (EC) is an aggressive malignancy, leading to a weak overall survival rate (10% ~20%) [1]. EC evolves into the eighth most common cancer and the sixth cause of cancer-related death [2]. According to the cell types involved, EC can be divided into esophageal adenocarcinoma (EAC) and esophageal squamous cell carcinoma (ESCC) [3]. ESCC shows greater geographic diversity in morbidity, mortality and sex ratios, especially in Eastern and Asian countries [4,5]. Risk factors for ESCC are thought to be related to diet, lifestyle and genetic polymorphisms [6]. However, the complex molecular mechanisms of ESCC initiation and development have not been fully understood. Therefore, there is an absolute need to improve medical treatment by identifying novel therapeutic targets.

With the development of high-throughput sequencing technique, a growing number of circular RNAs (circRNAs) closely linked to cancers have been identified [7]. CircRNAs are a new type of non-coding RNAs formed by back-splicing without 5’ cap and 3’ poly-A tail [8], which is different from linear mRNAs. Thousands of circRNAs are abundant, relatively stable and widely expressed in eukaryotic cells [9,10].

Recently, the association of circRNAs with the development of ESCC has been frequently reported, such as circ_100873, circ_100876 and circ_0067934 [11-13]. These circRNAs were associated with lymphatic metastasis, proliferation and cell cycle in ESCC, suggesting that circRNAs are vital regulators to participate in the development of ESCC. circ_DLG1, also named circ_0007203, is back-spliced from DLG1. A previous study suggested that circ_DLG1 was expressed with a high level in ESCC patients, associated with the TNM stage and could be a diagnostic factor [14]. However, the specific role of circ_DLG1 and potential functional mechanisms are not elucidated.

Mitogen-Activated Protein Kinase Kinase Kinase 9 (MAP3K9) is located in 14q24.3-q31 that encodes a MAPK kinase kinase belonging to a protein kinase signal transduction cascade [15]. MAPKs function in a wide range of cellular processes, including cell differentiation, proliferation and movability [16]. Genomic profiling about esophageal tissues and normal tissues predicted that MAP3K9 might play a substantial role in susceptibility and development of EC [17]. But the relevant research of MAP3K9 in ESCC is still limited.

MicroRNAs (miRNAs) are also a kind of non-coding RNAs with ~22 nucleotides in length that induce post-transcriptional gene silencing [18]. MiRNAs are indispensable involving in the circRNA-miRNA-mRNA regulatory network in human diseases [19]. Among these miRNAs, miR-338-3p is a widely regulated factor in diverse types of disease and cancer [20,21], including ESCC [22]. Therefore, the further excavation of miR-338-3p function and the exploration of the relevant action mechanism in ESCC are important to enrich its role.

This study monitored the expression of circ_DLG1 in ESCC tissues, plasma and cells. We also investigated the function of circ_DLG1 in cell proliferation, cycle, migration and invasion in ESCC and constructed the circ_DLG1/miR-338-3p/MAP3K9 functional network. Besides, the classical MAPK/ERK pathway was verified to participate in circ_DLG1 regulatory mode. Our study presented a novel mechanism to understand the pathogenesis of ESCC.

Materials And Methods

Experimental samples

Tissue samples, including ESCC tumor tissues (n=44) and adjacent normal tissues (n=44) from ESCC patients, and blood samples, including ESCC blood (n=26) and normal blood (n=26) from ESCC patients or healthy subjects, were collected from The First Affiliated Hospital of Xiamen. The written informed consent was signed by every participant. The excised tissues were frozen by liquid nitrogen and preserved in -80℃ conditions. The plasma was isolated from blood samples and stored at -80℃ for further detection. This research was approved by the Ethics Committee of The First Affiliated Hospital of Xiamen.

Cell lines

Human ESCC cell lines, including EC9706, KYSE30 and KYSE450, and normal esophageal squamous epithelial cells (HET-1A) were purchased from Bena Culture Collection (Suzhou, China). Another ESCC cell line TE-8 was purchased from SUER Technology Co., Ltd. (Shanghai, China). In line with the instructions, EC9706 and HET-1A cells were maintained in 90% Dulbecco's Modified Eagle Medium (DMEM; Gibco, Grand Island, NY, USA) containing 10% fetal bovine serum (FBS; Gibco). KYSE30, KYSE450 and TE-8 cells were cultured in 90% Roswell Park Memorial Institute 1640 (RPMI 1640; Gibco) containing 10% FBS (Gibco). All cells were stored at 37°C conditions containing 5% CO_2.

Quantitative real-time polymerase chain reaction (qRT-PCR)

Total RNA was extracted using the Total RNA Miniprep Kit (Sigma-Aldrich, St. Louis, MO, USA) from tissues and cells or using GenElute Plasma/Serum RNA Purification Mini Kit (Sigma-Aldrich) from plasma. After the detection of availability, the RNA was reversely transcribed into cDNA using Transcriptor High Fidelity cDNA Synthesis Kit (Roche, Basel, Switzerland) or MystiCq microRNA cDNA Synthesis Mix (Sigma-Aldrich). Afterwards, KiCqStart SYBR Green qPCR ReadyMix (Sigma-Aldrich) was utilized to conducted qRT-PCR amplification reaction under Bio-Rad CFX96 (Bio-Rad, Hercules, CA, USA). The relative expression was normalized by glyceraldehyde 3-phosphate dehydrogenase (GAPDH) or U6 and calculated using the $2^{-\Delta\Delta Ct}$ method. The primers were used in this study, including circ_DLG1, forward: 5'-AAACGAGAGATAAAGGGCTTCT-3' and reverse: 5'- ACTGCTTTAGAAACTGGGGAGT-3'; DLG1, forward: 5'-gtggatcattca aag cagtgtga-3' and reverse: 5'-aggctggcaatctcccaagt-3'; miR-338-3p, forward: 5'-ATCCAGTGCGTGTCGTGG-3' and reverse: 5'-TGCTTCCAGCATCAGTGAT-3'; MAP3K9, forward: 5'-GAGTGCGGCAGGGAC GTAT-3' and reverse: 5'-CCCCATAGCTCCACACATCAC-3'; GAPDH, forward: 5'-GAGTCCACTGGCGTCTTCAC-3' and reverse: 5'- ATCTTGAGGCTGTTGTCATACTTCT-3'; U6, forward: 5'-CTCGCTTCGGCAGCACATA-3' and reverse: 5'-CGCTTCACGAATTTGCGTG-3'.

CircRNA stability detection

RNase R treatment was performed as follows: 2 μg of total RNA was diluted in 10 μl of water with or without 2 $U{\cdot}mg^{-1}$ RNase R and 2 μl of enzyme buffer (Epicenter, Madison, WI, USA), then incubated 15 min at 37°C and then used for qRT-PCR.

Cell transfection

Small interference RNA (siRNA) targeting circ_DLG1 (si-circ_DLG1) (Ribobio, Guangzhou, China) was used for circ_DLG1 knockdown, and siRNA negative control (si-NC) was used as a reference. Circ_DLG1 overexpression (circ_DLG1) was assembled by BersinBio Co., Ltd. (Guangzhou, China) using their commercial expression vector, and empty vector (Vector) served as control. Overexpression vector pcDNA3.1 containing MAP3K9 fragment (Sangon Biotech, Shanghai, China) was used for MAP3K9 overexpression (MAP3K9), empty pcDNA3.1 vector (pcDNA) as the reference. MiR-338-3p mimics or inhibitors (miR-338-3p or anti-miR-338-3p) (Ribobio) were used for miR-338-3p enrichment or inhibition, miR-NC or anti-miR-NC as the respective reference. Lentivirus short-hairpin RNA against circ_DLG1 (sh-

circ_DLG1) (Sangon Biotech) was used for circ_DLG1 stable knockdown, sh-NC as the reference. Cell transfection was conducted using Lipofectamine 3000 (Invitrogen, Carlsbad, CA, USA).

Cell cycle detection

Cell cycle was detected using a Cell Cycle Analysis kit (Beyotime, Shanghai, China) following the instructions. At 48 h post-transfection, TE-8 and KYSE450 cells were washed twice with phosphate buffered saline (PBS), trypsinized and centrifuged at 1,500 × g for 5 min at 4℃. Then, cells were exposed to 100 μl of RNase A for 30 min at 37℃ and next stained with 400 μl propidium iodide (PI) for 30 min at 4℃ in the dark. Finally, the cells were analyzed using a FACSCalibur system (Beckman Coulter, Brea, CA, USA).

Cell proliferation analysis

After transfection, TE-8 and KYSE450 cells were seeded into 96-well plates at a density of 5×10^3 cells/well and placed at 37℃ containing 5% CO_2. Afterwards, 10 μg MTT (Beyotime) was added into each well at the specific time points (0, 1, 2 and 3 d) and incubated for a further 4 h. Next, 50 μl dimethylsulfoxide (DMSO) (Beyotime) was used to dissolve formazan. Eventually, cell proliferation was analyzed by examining the absorbance at 490 nm under a microplate reader (Thermo Fisher Scientific, Waltham, MA, USA).

Cell migration and invasion analysis

For migration assay, TE-8 and KYSE450 cells were seeded into the top of transwell chambers with 8.0-μm pore membranes in 24-well plates (Corning Incorporated, Corning, NY, USA). For invasion assay, however, the chambers were pre-assembled with a thin layer of Matrigel (Corning Incorporated) prior to the cells were seeded. Meanwhile, RPMI 1640 fresh medium containing 10% FBS was added into the bottom of chambers. After incubation for 24 h, the bottom-surfaced cells were fixed with 4% paraformaldehyde and stained with 0.1% crystal violet (Beyotime) for 20 min. Finally, the cells were photographed and viewed under a microscope (Olympus, Tokyo, Japan).

Western blot

Total protein was extracted using the radioimmunoprecipitation assay (RIPA) buffer (Beyotime) and quantified by BCA assay kit (Beyotime). Then, proteins (20 μg/sample) were separated by 10% sodium dodecyl sulfate-polyacrylamide gel electrophoresis (SDS-PAGE) and transferred onto polyvinylidene fluoride (PVDF) membranes (Bio-Rad). Next, the membranes were suffered blockage buffer and incubated at 4℃ overnight within the primary antibodies against MAP3K9 (ab228752; Abcam, Cambridge, MA. USA), p38 (ab197348; Abcam), phosphor p38 (p-p38; ab4822; Abcam), extracellular signal-regulated kinase 1 and 2 (ERK1/2) (ERKs; ab184699; Abcam), phosphor ERKs (p-ERKs; ab214036; Abcam), Ki67 (ab16667; Abcam) and GAPDH (ab9485; Abcam). Afterwards, the membranes were probed

with the horseradish peroxidase (HRP)-labeled secondary antibodies (ab205718; Abcam). The protein blots on the membranes were emerged using the chemiluminescence kit (Beyotime).

Bioinformatics prediction and dual-luciferase reporter assay

The online bioinformatics tool starBase (http://starbase.sysu.edu.cn/) was used to analyze the putative targeted genes.

Wild-type sequences of circ_DLG1 containing the miR-338-3p binding site and mutant-type sequences of circ_DLG1 containing the miR-338-3p mutated binding site were inserted into the pGL4 vector (Promega, Madison, WI, USA), named as circ_DLG1-wt and circ_DLG1-mut. Likewise, wild-type sequences of MAP3K9 containing the miR-338-3p binding site and mutant-type sequences of MAP3K9 containing the miR-338-3p mutated binding site were cloned into the pGL4 vector, named as MAP3K9-wt and MAP3K9-mut. TE-8 and KYSE450 cells seeded into 24-well plates were co-transfected with 50 nM miR-338-3p or miR-NC and circ_DLG1-wt, circ_DLG1-mut, MAP3K9-wt or MAP3K9-mut using Lipofectamine 3000. The luciferase activity was examined using the dual-luciferase reporter assay kit (Promega) after 48-h transfection.

Animal experiments

Animal procedures were conducted conforming to the Animal Care and Use Committee of The First Affiliated Hospital of Xiamen. 5-week-old nude mice (Female, n=8) were purchased from the Animal Core Facility, SIBCB (Shanghai, China). TE-8 cells stably transfected with sh-circ_DLG1 or sh-NC were subcutaneously implanted into the right flank of mouse back. Tumor volume was recorded every 5 d using the formula: length × width^2 × 0.5. Tumors were excised after 30 d.

Statistical analysis

Statistical analysis was performed using SPSS 21.0 software (IBM Corp., Armonk, NY, USA). The linear dependence was analyzed by Spearman's correlation analysis. All data were collected from three independent experiments and displayed as mean ± standard deviation. The Student's *t*-test was applied to analyze the differential significance between two groups, and analysis of variance (ANOVA) was applied to analyze significance among more than two groups, followed by the Tukey correction for multiple comparisons. $P < 0.05$ was considered to be statistically significant.

Result

The expression of circ_DLG1 was upregulated in ESCC tissues, plasma and cells

The examination of the expression of circ_DLG1 was conducted using qRT-PCR in ESCC tissues, plasma and cells. Consistently, the expression of circ_DLG1 was aberrantly elevated in ESCC tumor tissues, plasma from patients with tumor and ESCC cell lines (EC9706, KYSE30, TE-8 and KYSE450) relative to adjacent normal tissues, plasma from normal subjects and Normal esophageal squamous epithelial cells

(HET-1A), respectively (Figure 1A, 1B and 1C). The data suggested that circ_DLG1 might play specific roles in ESCC.

Circ_DLG1 regulated cell cycle and cell proliferation in KYSE450 and TE-8 cells

The effects of circ_DLG1 on proliferation were explored to ensure the biological function of circ_DLG1 using gain- or loss-function assay. Firstly, the stability of circ_DLG1 was examined using RNase R, and the result presented that RNase R treatment hardly affected the expression of circ_DLG1 but significantly diminished the expression of linear mRNA (DLG1), suggesting that circ_DLG1 stably existed in KYSE450 and TE-8 cells (Figure 2A and 2B). Next, the efficiency of circ_DLG1 knockdown or overexpression was checked, and the data displayed that the expression of circ_DLG1 was notably decreased in TE-8 and KYSE450 cells with the transfection of si-circ_DLG1 relative to si-NC but increased with the transfection of circ_DLG1 relative to NC (Figure 2C and 2D). For cell cycle detection, circ_DLG1 knockdown prominently reduced the number of S-phase cells compared with control, indicating that circ_DLG1 knockdown repressed cell transition from G1 to S and G2 (Figure 2E and 2G). On the contrary, circ_DLG1 overexpression increased the number of S-phase cells in TE-8 and increased the number of G2-phase cells in KYSE450, indicating that circ_DLG1 overexpression accelerated the cell transition from G1 to S and G2 (Figure 2I and 2K). Besides, circ_DLG1 knockdown pronouncedly inhibited the proliferation of TE-8 and KYSE450 cells (Figure 2F and 2H), while circ_DLG1 overexpression significantly promoted the proliferation of TE-8 and KYSE450 cells (Figure 2J and 2L). These analyses summarized that circ_DLG1 promoted cell cycle and proliferation.

Circ_DLG1 regulated cell migration and invasion in TE-8 and KYSE450 cells

Next, we explored the effects of circ_DLG1 on cell migration and invasion using transwell assay. The result exhibited that the number of migrated and invaded cells was markedly declined in TE-8 and KYSE450 cells transfected with si-circ_DLG1 compared with si-NC (Figure 3A and 3B), while the number of migrated and invaded cells was markedly reinforced in TE-8 and KYSE450 cells transfected with circ_DLG1 compared with Vector (Figure 3C and 3D). The data showed that circ_DLG1 promoted cell migration and invasion.

MAP3K9 was highly expressed in ESCC tissues and cells

The expression of MAP3K9 was strengthened in ESCC tissues (n=44) compared with normal tissues (n=44) at both mRNA and protein levels (Figure 4A and 4B). Interestingly, MAP3K9 expression was positively correlated with circ_DLG1 expression in ESCC tissues (Figure 4C). Likewise, the expression of MAP3K9 was also enhanced in TE-8 and KYSE450 cells relative to that in HET-1A cells at both mRNA and protein levels (Figure 4D and 4E). The data hinted that MAP3K9 was aberrantly upregulated in ESCC.

MAP3K9 overexpression rescued the effects of circ_DLG1 knockdown on cell cycle, proliferation, migration and invasion

TE-8 and KYSE450 cells were introduced with si-circ_DLG1 or si-circ_DLG1+MAP3K9, si-NC or si-circ_DLG1+pcDNA as the control. We found that the expression of MAP3K9 was decreased in TE-8 and KYSE450 cells transfected with si-circ_DLG1 but recovered in cells transfected with si-circ_DLG1+MAP3K9 at both mRNA and protein levels (Figure 5A and 5B), indicating the transfection efficiency was acceptable. Functionally, the cell transition from G1 to S and G2 suppressed in TE-8 cells transfected with si-circ_DLG1 was recovered by the transfection of si-circ_DLG1+MAP3K9 (Figure 5C). Similarly, circ_DLG1 knockdown-inhibited proliferation of TE-8 cells was significantly encouraged in cells transfected with si-circ_DLG1+MAP3K9 (Figure 5D). The presentation of cell cycle and cell proliferation in KYSE450 cells with transfection was consistent with that in TE-8 cells (Figure 5E and 5F). The abilities of migration and invasion were suppressed in si-circ_DLG1 transfected TE-8 and KYSE450 cells but elevated in cells transfected with si-circ_DLG1+MAP3K9 (Figure 5G and 5H). These results indicated that MAP3K9 overexpression could promote cell cycle, proliferation, migration and invasion, which was inhibited by circ_DLG1 knockdown.

MiR-338-3p was a link between circ_DLG1 and MAP3K9

MiR-338-3p was predicted to be a target of circ_DLG1 with a special targeting site by the online tool starBase 3.0 (Figure 6A). Then, the dual-luciferase reporter assay was performed to confirm this prediction, and the data showed that miR-338-3p reintroduction markedly weakened the luciferase activity in TE-8 and KYSE450 cells transfected with circ_DLG1-wt but not circ_DLG1-mut relative to miR-NC (Figure 6B and 6C). Not surprisingly, the expression of miR-338-3p was notably enhanced in TE-8 and KYSE450 cells with circ_DLG1 knockdown but notably impaired in TE-8 and KYSE450 cells with circ_DLG1 overexpression (Figure 6D). Subsequently, the expression of miR-338-3p was examined in ESCC tissues and cells, and we noticed that the content of miR-338-3p was remarkably lower in tumor tissues than that in normal tissues (Figure 6E). Besides, the content of miR-338-3p in TE-8 and KYSE450 cells was also lessened compared with that in HET-1A cells (Figure 6F). In addition, miR-338-3p expression was negatively correlated with circ_DLG1 expression in ESCC tissues (Figure 6G). Interestingly, MAP3K9 was a putative target of miR-338-3p with special binding sites between its 3'UTR and miR-338-3p, which was forecasted by the online tool starBase 3.0 (Figure 6H). In addition, their targeted relationship was verified by dual-luciferase reporter assay (Figure 6I and 6J). Then, TE-8 and KYSE450 cells were transfected with miR-338-3p or anti-miR-338-3p, miR-NC or anti-miR-NC as the control. The expression of miR-338-3p was elevated in TE-8 and KYSE450 cells with miR-338-3p transfection but depleted with anti-miR-338-3p transfection (Figure 6K and 6L). While the expression of MAP3K9 was repressed in TE-8 and KYSE450 cells with miR-338-3p transfection but stimulated with anti-miR-338-3p transfection at both mRNA and protein levels (Figure 6M and 6N). Moreover, miR-338-3p expression was negatively correlated with MAP3K9 expression at the mRNA level in ESCC tissues (Figure 6O). These data suggested that miR-338-3p might be a link between circ_DLG1 and MAP3K9.

Circ_DLG1 knockdown functioned by weakening the expression of MAP3K9 via targeting miR-338-3p

The data from qRT-PCR and western blot presented that the expression of MAP3K9 was significantly reduced in TE-8 and KYSE450 cells with the transfection of si-circ_DLG1 but obviously enhanced in TE-8 and KYSE450 cells with the transfection of si-circ_DLG1+anti-miR-338-3p (Figure 7A and 7B), indicating that circ_DLG1 regulated MAP3K9 expression by mediating miR-338-3p. Functionally, circ_DLG1 knockdown-arrested cell cycle was promoted in TE-8 and KYSE450 cells transfected with si-circ_DLG1+anti-miR-338-3p (Figure 7C and 7E). Besides, the proliferation of TE-8 and KYSE450 cells was blocked with si-circ_DLG1 transfection but notably restored with si-circ_DLG1+anti-miR-338-3p transfection (Figure 7D and 7F). Moreover, the capacities of cell migration and invasion blocked in TE-8 and KYSE450 cells transfected with si-circ_DLG1 were partially elevated in cells transfected with si-circ_DLG1+anti-miR-338-3p (Figure 7G and 7H). These data exhibited that circ_DLG1 knockdown blocked the malignant activities by impairing MAP3K9 via enriching miR-338-3p.

The circ_DLG1/miR-338-3p/MAP3K9 axis participated in ESCC progression via regulating the MAPK/ERK pathway

MAPK/ERK signaling pathway was frequently mentioned in human diseases, including cancer. Further, we explored whether this pathway was involved in the circ_DLG1/miR-338-3p/MAP3K9 axis in ESCC. The data from western blot showed that the levels of p-p38 and p-ERKs were declined in TE-8 and KYSE450 cells with si-circ_DLG1 transfection, while the transfection of si-circ_DLG1+anti-miR-338-3p or si-circ_DLG1+MAP3K9 substantially recovered the levels of p-MAPK and p-ERKs declined by si-circ_DLG1 transfection in TE-8 and KYSE450 cells (Figure 8A and 8B). The regular expression change of p-p38 and p-ERKs suggested that MAPK/ERK pathway was involved in the circ_DLG1/miR-338-3p/MAP3K9 regulatory axis.

Circ_DLG1 knockdown blocked tumor growth *in vivo* by modulating miR-338-3p and MAP3K9

TE-8 cells with the transfection of sh-circ_DLG1 or sh-NC were injected into nude mice to monitor the role of circ_DLG1 *in vivo*. The note presented that the tumor volume in the sh-circ_DLG1 group was significantly lower than that in the sh-NC group (Figure 9A). At 30 d after injection, all mice were killed, and the tumor was excised. The expression of proliferation activity-related protein Ki67 at the protein level was markedly decreased in the sh-circ_DLG1 group relative to that in the sh-NC group (Figure 9B), hinting that circ_DLG1 knockdown inhibited tumor growth. Besides, circ_DLG1 knockdown also impaired the tumor weight compared to control (Figure 9C). The expression analyses displayed that the expression of circ_DLG1 was reduced in the excised tumor tissues from the sh-circ_DLG1 group relative to the sh-NC group, while the expression of miR-338-3p was enhanced (Figure 9D and 9E). The expression of MAP3K9 at both mRNA and protein levels was unsurprisingly depleted in tumor tissues from the sh-circ_DLG1 group relative to the sh-NC group (Figure 9F and 9G). The data concluded that circ_DLG1 knockdown suppressed tumor growth *in vivo* by upregulating miR-338-3p and downregulating MAP3K9.

Discussion

The identification of circRNAs in ESCC helps to broaden people's eyes to understand ESCC progression with complex pathogenesis, and circRNAs are promising biomarkers for ESCC diagnosis and prognosis [23]. Data from the present study indicated that circ_DLG1 was excessive in ESCC tissues, plasma and cells. Functional analyses revealed that circ_DLG1 knockdown inhibited cell cycle, proliferation, migration and invasion *in vitro* and attenuated tumor growth *in vivo*. Regarding the potential mechanisms, this paper provided evidence that circ_DLG1 played its functioned by regulating the MAPK/ERK pathway following the miR-338-3p/MAP3K9 axis. The present study provided vital clues to enrich the functional roles of circ_DLG1 in ESCC and presented a theoretical basis for its application in ESCC therapeutic strategy.

Although the important role of circRNAs in cancer has been clarified, the research on circRNAs in cancer is still limited. A previous study led us to know that circ_DLG1 was abundantly expressed in ESCC tissues and cell lines, and circ_DLG1 underexpression effectively suppressed cell proliferation and colony formation [14]. However, the more biological functions of circ_DLG1 and its associated regulatory pathway involved in the ESCC development have not been mentioned. The presented study also conveyed that the abundance of circ_DLG1 was strengthened in ESCC tissues, plasma and cells. Functionally, circ_DLG1 knockdown significantly weakened cell cycle, proliferation, migration and invasion of ESCC cells, while circ_DLG1 overexpression presented the opposite effects. These results hinted that circ_DLG1 might act as a tumor promoter in ESCC.

MAP3K9, also well known as mixed-lineage kinase 1 (MLK1), was previously classified into an oncogene [24]. The carcinogenic effects of MAP3K9 have been characterized in numerous cancers. For example, miR-7, miR-490-5p and miR-148a exerted their tumor inhibitor role in pancreatic cancer [25], pharyngolaryngeal cancer [26] and cutaneous squamous cell carcinoma [27] by targeting MAP3K9, respectively. In ESCC, a recent study also concluded that miR-148a depleted the expression of MAP3K9 to block the development of ESCC [28]. These findings emphasized the consistent carcinogenic role of MAP3K9 in diverse cancers. Uniformly, MAP3K9 was aberrantly upregulated in ESCC tissues and cells in this study, and MAP3K9 downregulation sequestered cell cycle, proliferation, migration and invasion. Besides, MAP3K9 overexpression rescued the effects of circ_DLG1 knockdown.

The most studied function of circRNAs is acting as miRNA sponges to modulate the expression of downstream mRNA, thus participating in biological processes, such as tumor development [29]. Here, miR-338-3p was identified as a target of circ_DLG1, and miR-338-3p directly bound to MAP3K9. Besides, circ_DLG1 knockdown depleted the expression of MAP3K9 by upregulating miR-338-3p, suggesting that circ_DLG1 regulated MAP3K9 by adsorbing miR-338-3p. The data from previous studies displayed that miR-338-3p was notably downregulated in ESCC tissues [22,30]. However, the biological functions of miR-338-3p have not been explored. Our study functionally presented that miR-338-3p deficiency reversed the effects of circ_DLG1 knockdown, suggesting that miR-338-3p was a tumor suppressor in ESCC.

Moreover, the MAPK/ERK signaling pathway was confirmed to be involved in the circ_DLG1/miR-338-3p/MAP3K9 regulatory axis in this study. The activation of the MAPK/ERK signaling pathway was closely

connected with the development of tumors [31,32]. MLK was identified as an upstream modulator of MAPKs to activate p38 MAPK pathway, MEK pathway or ERK pathway [25]. Hence, the experiments were performed to detect whether MAPK signaling pathway was involved in the circ_DLG1/miR-338-3p/MAP3K9 regulatory axis. Interestingly, circ_DLG1 knockdown weakened the expression of p-p38 and p-ERKs, while MAP3K9 overexpression or miR-338-3p inhibition reversed these effects, suggesting that the p38 MAPK/ERK pathway was associated with circ_DLG1 action mode in ESCC.

Conclusion

Taken together, circ_DLG1 was aberrantly upregulated in ESCC tissues, plasma and cells. Circ_DLG1 knockdown suppressed malignant cellular activities *in vitro* and tumor growth *in vivo* by mediating miR-338-3p/MAP3K9 axis via inactivating the MAPK/ERK signaling pathway. Our study enriched the role of circ_DLG1 and provided a novel functional mechanism of circ_DLG1 to defend ESCC.

Declarations

Acknowledgement

Not applicable

Funding

No funding was received.

Availability of data and materials

The datasets used and analyzed during this study are available from the corresponding author on reasonable request.

Ethics approval and consent for publication

All patients included in the presents study provided written informed consent prior to their inclusion. The study was approved by the ethics committee of the The First Affiliated Hospital of Xiamen.

Authors' contribution

Conceptualization and Methodology: Bing Zhu and Zhaofeng Ning; Formal analysis and Data curation: Xiaodong Wang, Zhaoxia Li and Chunxia Zhang; Validation and Investigation: Yixuan Yang, Bing Zhu and Linchun Wen; Writing - original draft preparation and Writing - review and editing: Yixuan Yang, Bing Zhu and Bing Zhu; Approval of final manuscript: all authors

Patients consent for publication

Not applicable

Disclosure of interest

The authors declare that they have no financial conflict of interest.

References

1. Sugihara H, Ishimoto T, Miyake K, Izumi D, Baba Y, Yoshida N, et al. Noncoding RNA Expression Aberration Is Associated with Cancer Progression and Is a Potential Biomarker in Esophageal Squamous Cell Carcinoma. Int J Mol Sci. 2015;16:27824-34.
2. Jemal A, Bray F, Center MM, Ferlay J, Ward E, Forman D. Global cancer statistics. CA Cancer J Clin. 2011;61:69-90.
3. Tungekar A, Mandarthi S, Mandaviya PR, Gadekar VP, Tantry A, Kotian S, et al. ESCC ATLAS: A population wide compendium of biomarkers for Esophageal Squamous Cell Carcinoma. Sci Rep. 2018;8:12715.
4. Testa U, Castelli G, Pelosi E. Esophageal Cancer: Genomic and Molecular Characterization, Stem Cell Compartment and Clonal Evolution. Medicines (Basel). 2017;4:
5. Zeng H, Zheng R, Zhang S, Zuo T, Xia C, Zou X, et al. Esophageal cancer statistics in China, 2011: Estimates based on 177 cancer registries. Thorac Cancer. 2016;7:232-7.
6. Dotto GP, Rustgi AK. Squamous Cell Cancers: A Unified Perspective on Biology and Genetics. Cancer Cell. 2016;29:622-37.
7. Geng Y, Jiang J, Wu C. Function and clinical significance of circRNAs in solid tumors. J Hematol Oncol. 2018;11:98.
8. Chen LL, Yang L. Regulation of circRNA biogenesis. RNA Biol. 2015;12:381-8.
9. Jeck WR, Sorrentino JA, Wang K, Slevin MK, Burd CE, Liu J, et al. Circular RNAs are abundant, conserved, and associated with ALU repeats. RNA. 2013;19:141-57.
10. Zhang Z, Xie Q, He D, Ling Y, Li Y, Li J, et al. Circular RNA: new star, new hope in cancer. BMC Cancer. 2018;18:834.
11. Zheng B, Wu Z, Xue S, Chen H, Zhang S, Zeng T, et al. hsa_circRNA_100873 upregulation is associated with increased lymphatic metastasis of esophageal squamous cell carcinoma. Oncol Lett. 2019;18:6836-44.
12. Cao S, Chen G, Yan L, Li L, Huang X. Contribution of dysregulated circRNA_100876 to proliferation and metastasis of esophageal squamous cell carcinoma. Onco Targets Ther. 2018;11:7385-94.
13. Xia W, Qiu M, Chen R, Wang S, Leng X, Wang J, et al. Circular RNA has_circ_0067934 is upregulated in esophageal squamous cell carcinoma and promoted proliferation. Sci Rep. 2016;6:35576.
14. Rong J, Wang Q, Zhang Y, Zhu D, Sun H, Tang W, et al. Circ-DLG1 promotes the proliferation of esophageal squamous cell carcinoma. Onco Targets Ther. 2018;11:6723-30.
15. Stark MS, Woods SL, Gartside MG, Bonazzi VF, Dutton-Regester K, Aoude LG, et al. Frequent somatic mutations in MAP3K5 and MAP3K9 in metastatic melanoma identified by exome sequencing. Nat

Genet. 2011;44:165-9.
16. Imajo M, Tsuchiya Y, Nishida E. Regulatory mechanisms and functions of MAP kinase signaling pathways. IUBMB Life. 2006;58:312-7.
17. Chen J, Guo L, Peiffer DA, Zhou L, Chan OT, Bibikova M, et al. Genomic profiling of 766 cancer-related genes in archived esophageal normal and carcinoma tissues. Int J Cancer. 2008;122:2249-54.
18. Creighton CJ, Benham AL, Zhu H, Khan MF, Reid JG, Nagaraja AK, et al. Discovery of novel microRNAs in female reproductive tract using next generation sequencing. PLoS One. 2010;5:e9637.
19. Rong D, Sun H, Li Z, Liu S, Dong C, Fu K, et al. An emerging function of circRNA-miRNAs-mRNA axis in human diseases. Oncotarget. 2017;8:73271-81.
20. Howe JRt, Li ES, Streeter SE, Rahme GJ, Chipumuro E, Russo GB, et al. MiR-338-3p regulates neuronal maturation and suppresses glioblastoma proliferation. PLoS One. 2017;12:e0177661.
21. Chun S, Du F, Westmoreland JJ, Han SB, Wang YD, Eddins D, et al. Thalamic miR-338-3p mediates auditory thalamocortical disruption and its late onset in models of 22q11.2 microdeletion. Nat Med. 2017;23:39-48.
22. Wu B, Li C, Zhang P, Yao Q, Wu J, Han J, et al. Dissection of miRNA-miRNA interaction in esophageal squamous cell carcinoma. PLoS One. 2013;8:e73191.
23. Fan L, Cao Q, Liu J, Zhang J, Li B. Circular RNA profiling and its potential for esophageal squamous cell cancer diagnosis and prognosis. Mol Cancer. 2019;18:16.
24. Hannes S, Abhari BA, Fulda S. Smac mimetic triggers necroptosis in pancreatic carcinoma cells when caspase activation is blocked. Cancer Lett. 2016;380:31-8.
25. Xia J, Cao T, Ma C, Shi Y, Sun Y, Wang ZP, et al. miR-7 Suppresses Tumor Progression by Directly Targeting MAP3K9 in Pancreatic Cancer. Mol Ther Nucleic Acids. 2018;13:121-32.
26. Abdeyrim A, Cheng X, Lian M, Tan Y. miR4905p regulates the proliferation, migration, invasion and epithelialmesenchymal transition of pharyngolaryngeal cancer cells by targeting mitogenactivated protein kinase kinasekinase 9. Int J Mol Med. 2019;44:240-52.
27. Luo Q, Li W, Zhao T, Tian X, Liu Y, Zhang X. Role of miR-148a in cutaneous squamous cell carcinoma by repression of MAPK pathway. Arch Biochem Biophys. 2015;583:47-54.
28. Zhang BX, Yu T, Yu Z, Yang XG. MicroRNA-148a regulates the MAPK/ERK signaling pathway and suppresses the development of esophagus squamous cell carcinoma via targeting MAP3K9. Eur Rev Med Pharmacol Sci. 2019;23:6497-504.
29. Zhang H, Shen Y, Li Z, Ruan Y, Li T, Xiao B, et al. The biogenesis and biological functions of circular RNAs and their molecular diagnostic values in cancers. J Clin Lab Anal. 2019;e23049.
30. Yang M, Liu R, Sheng J, Liao J, Wang Y, Pan E, et al. Differential expression profiles of microRNAs as potential biomarkers for the early diagnosis of esophageal squamous cell carcinoma. Oncol Rep. 2013;29:169-76.
31. Wang JL, Yang MY, Xiao S, Sun B, Li YM, Yang LY. Downregulation of castor zinc finger 1 predicts poor prognosis and facilitates hepatocellular carcinoma progression via MAPK/ERK signaling. J Exp

Clin Cancer Res. 2018;37:45.

32. Chen K, Liu MX, Mak CS, Yung MM, Leung TH, Xu D, et al. Methylation-associated silencing of miR-193a-3p promotes ovarian cancer aggressiveness by targeting GRB7 and MAPK/ERK pathways. Theranostics. 2018;8:423-36.

Figures

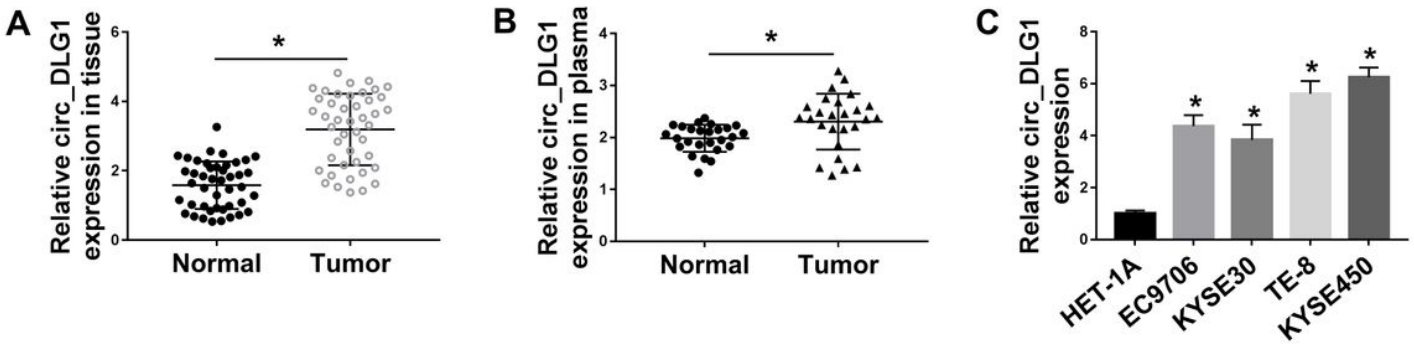

Figure 1

Circ_DLG1 was upregulated in ESCC tissues, plasma and cells. (A) The expression of circ_DLG1 in ESCC tumor tissues (n=44) and matched normal tissues (n=44) was detected by qRT-PCR. (B) The expression of circ_DLG1 in plasma from ESCC patients (n=26) and healthy subjects (n=26) was detected by qRT-PCR. (C) The expression of circ_DLG1 in ESCC cell lines (EC9706, KYSE30, TE-8 and KYSE450) and normal cell line (HET-1A) was detected by qRT-PCR. *P < 0.05.

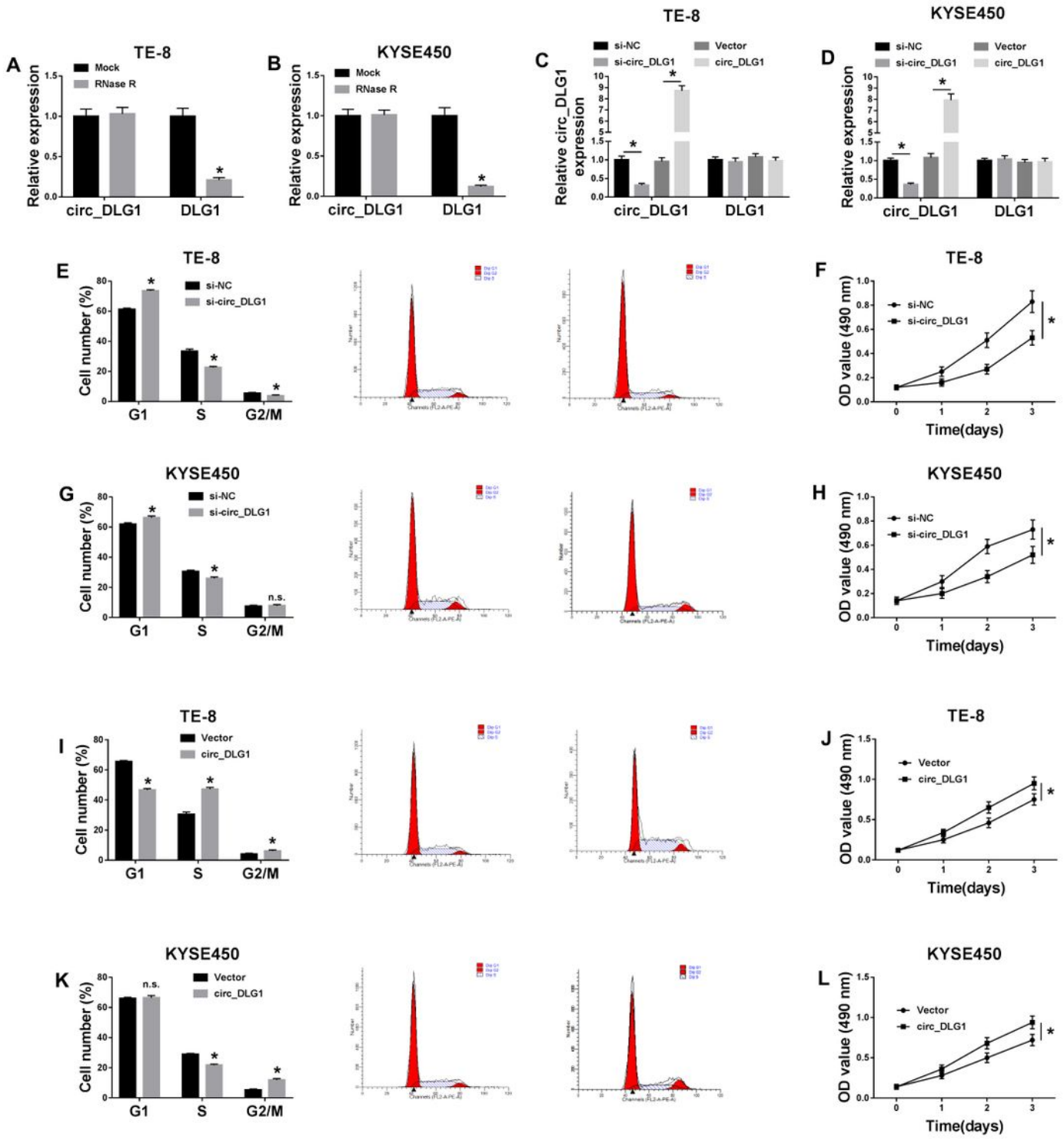

Figure 2

Circ_DLG1 regulated cell cycle and proliferation. (A and B) The stability detection of circ_DLG1 and its linear mRNA DLG1 was detected by qRT-PCR in TE-8 and KYSE450 cells treated with RNase R. (C and D) The efficiency of circ_DLG1 knockdown and overexpression was checked by qRT-PCR. (E) TE-8 cells with circ_DLG1 knockdown were subjected to flow cytometry analysis to evaluate cell cycle distribution. (F) The proliferation of TE-8 cells transfected with si-circ_DLG1 was assessed by MTT assay. (G) KYSE450

cells with circ_DLG1 knockdown were subjected to flow cytometry analysis to evaluate cell cycle distribution. (H) The proliferation of KYSE450 cells transfected with si-circ_DLG1 was assessed by MTT assay. (I) TE-8 cells with circ_DLG1 overexpression were subjected to flow cytometry analysis to evaluate cell cycle distribution. (J) The proliferation of TE-8 cells transfected with circ_DLG1 was assessed by MTT assay. (K) KYSE450 with circ_DLG1 overexpression were subjected to flow cytometry analysis to evaluate cell cycle distribution. (L) The proliferation of KYSE450 cells transfected with circ_DLG1 was assessed by MTT assay. *P < 0.05.

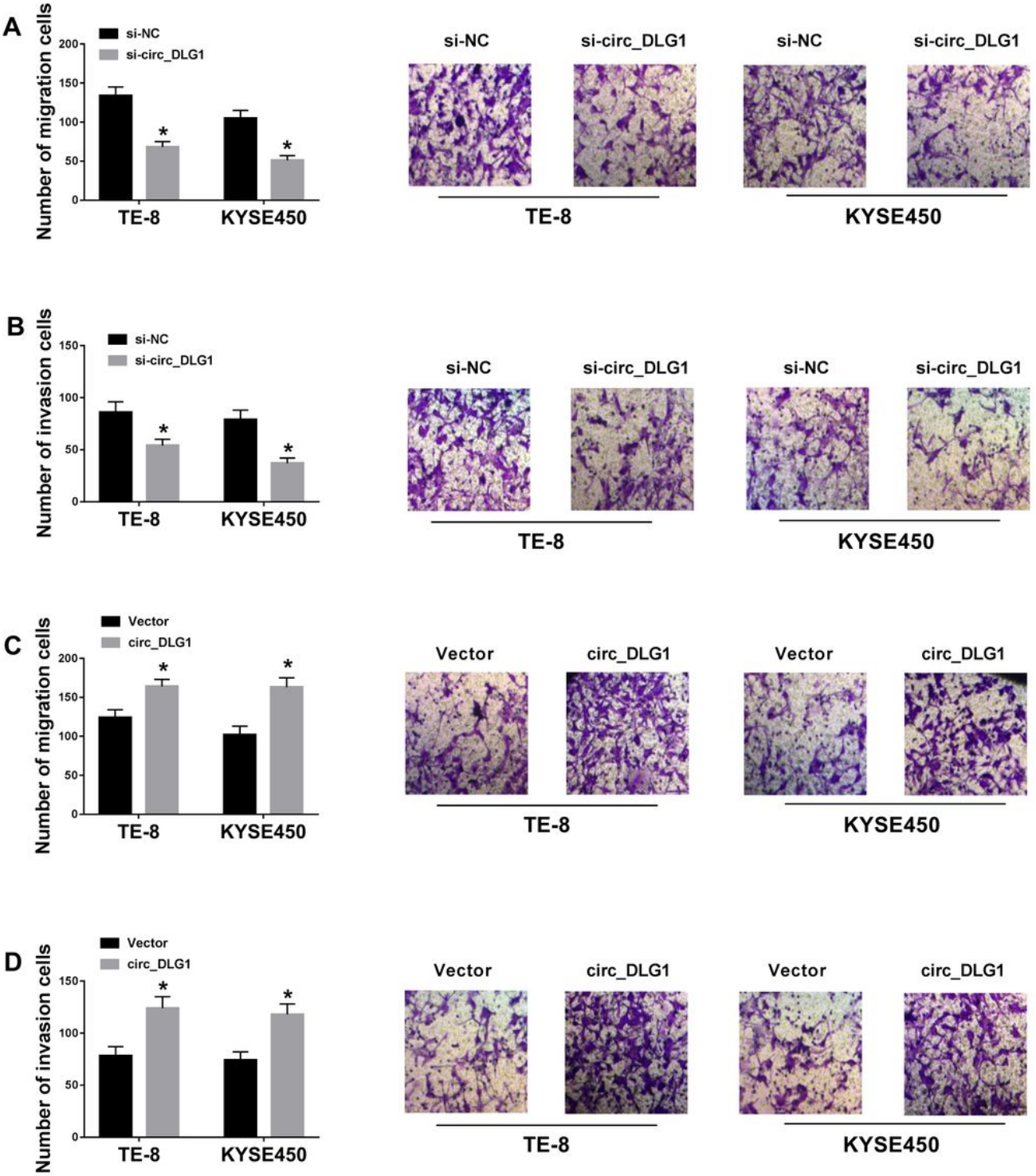

Figure 3

Circ_DLG1 regulated cell migration and invasion. (A and B) The migration and invasion of TE-8 and KYSE450 cells transfected with si-circ_DLG1 were monitored by transwell assay. (C and D) The migration and invasion of TE-8 and KYSE450 cells transfected with circ_DLG1 were determined by transwell assay. *P < 0.05.

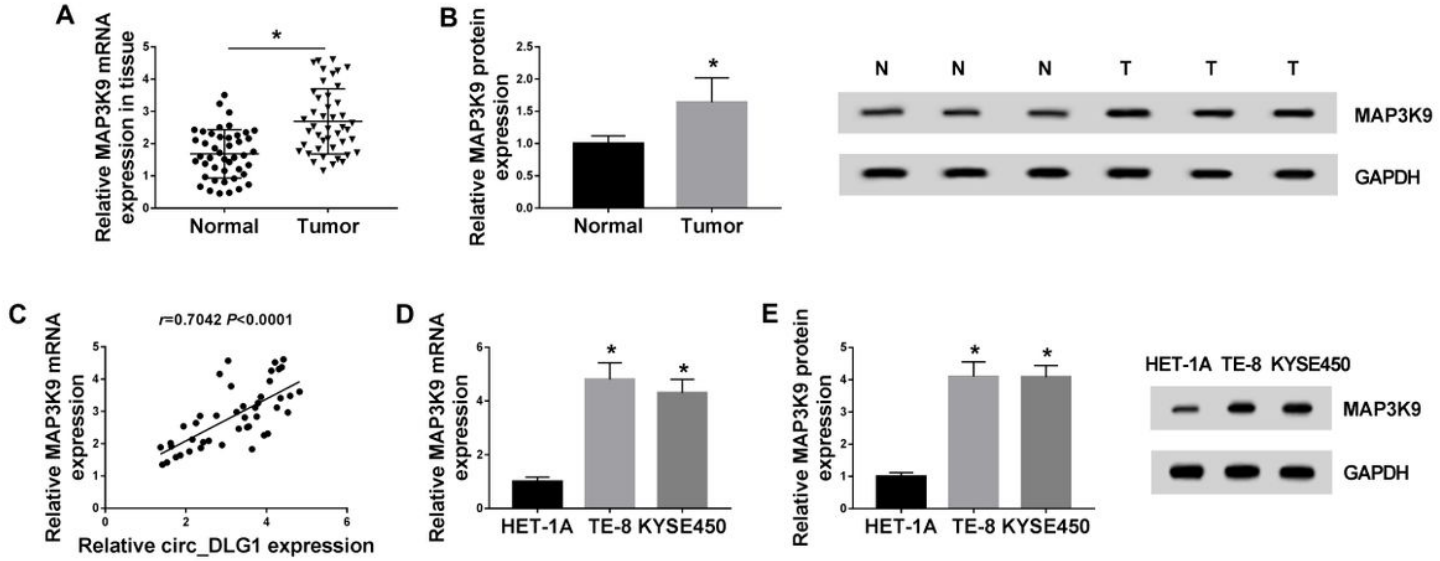

Figure 4

MAP3K9 was upregulated in ESCC tissues and cells. (A and B) The expression of MAP3K9 in tumor tissues (n=44) and normal tissues (n=44) was measured by qRT-PCR and western blot at both mRNA and protein levels. (C) The positive correlation between MAP3K9 expression and circ_DLG1 expression was analyzed by Spearman's correlation analysis. (D and E) The expression of circ_DLG1 in TE-8, KYSE450 and HET-1A cells was measured by qRT-PCR and western blot at both mRNA and protein levels. *P < 0.05.

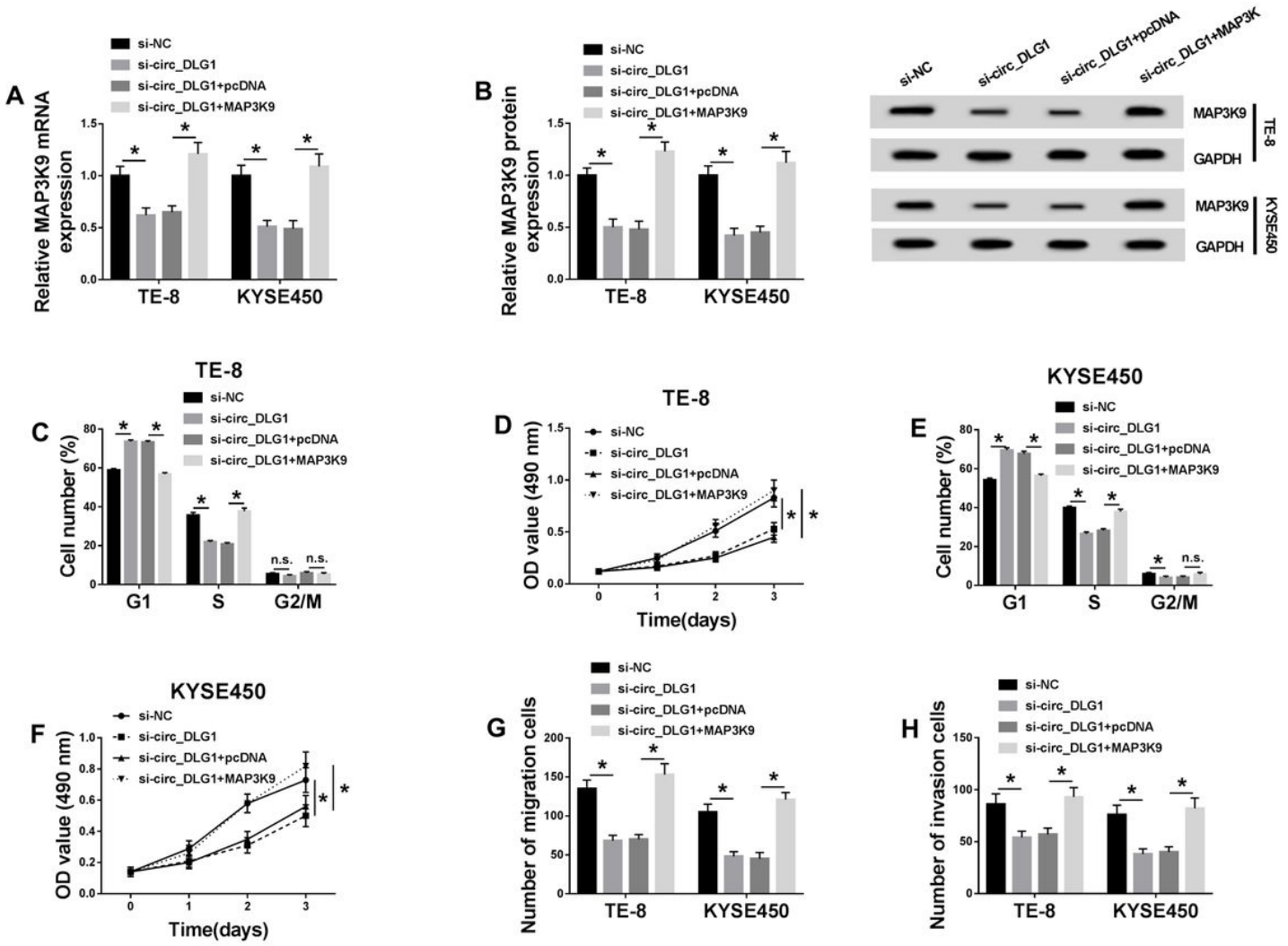

Figure 5

MAP3K9 overexpression promoted cell cycle, proliferation, migration and invasion blocked by circ_DLG1 knockdown. TE-8 and KYSE450 cells were transfected with si-circ_DLG1, si-NC, si-circ_DLG1+MAP3K9 or si-circ_DLG1+pcDNA. (A and B) The expression of MAP3K9 was checked in these cells by qRT-PCR and western blot. (C and D) Cell cycle and proliferation in TE-8 cells were investigated using flow cytometry assay and MTT assay, respectively. (E and F) Cell cycle and proliferation in KYSE450 cells were investigated using flow cytometry assay and MTT assay, respectively. (G and H) Cell migration and invasion were detected by transwell assay. *P < 0.05.

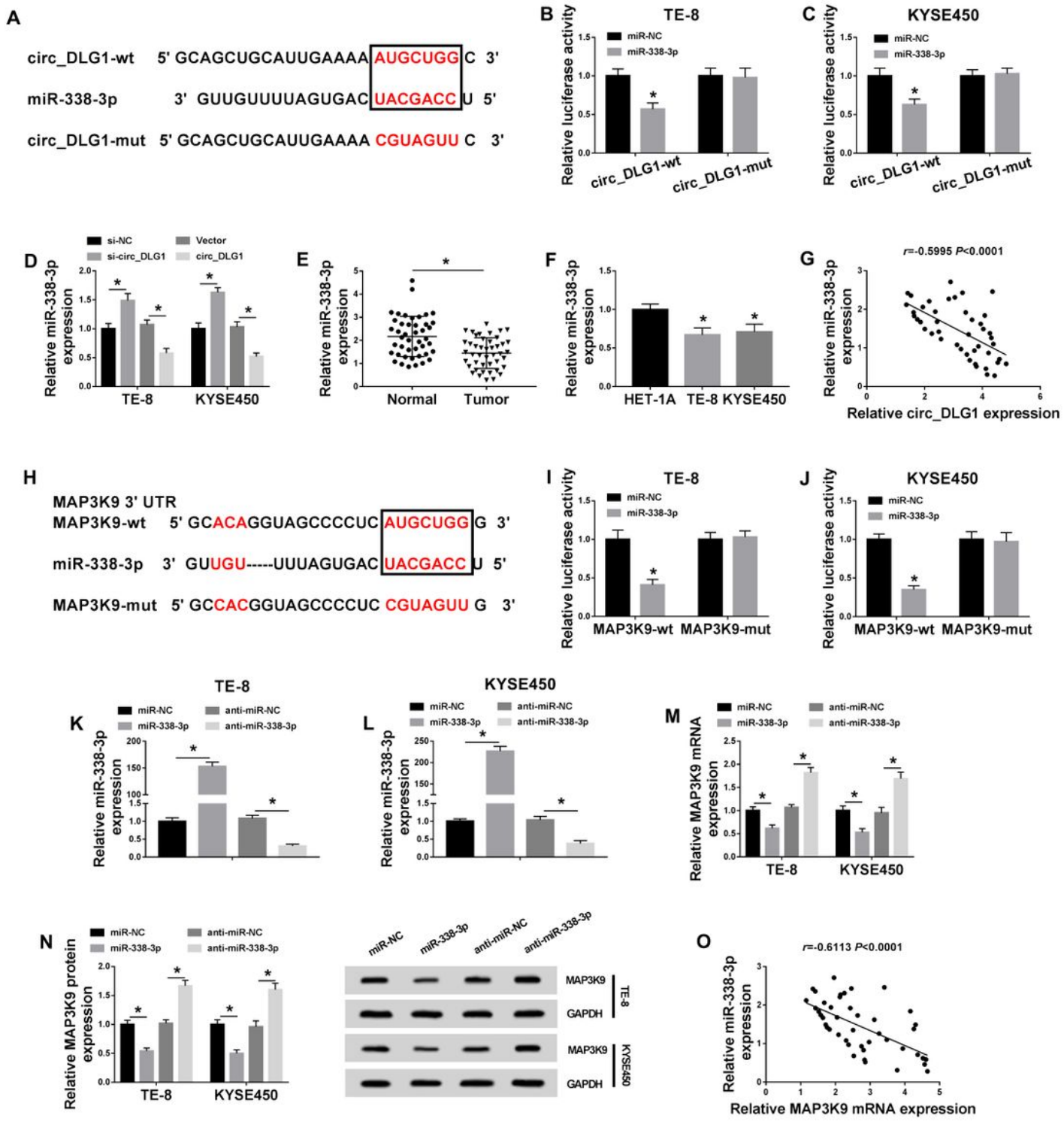

Figure 6

Circ_DLG1 targeted miR-338-3p, and miR-338-3p bound to MAP3K9. (A) MiR-338-3p was predicted as a target of circ_DLG1 by starBase. (B and C) The association between circ_DLG1 and miR-338-3p was verified by dual-luciferase reporter assay. (D) The expression of miR-338-3p in TE-8 and KYSE450 cells with circ_DLG1 knockdown or overexpression was measured by qRT-PCR. (E) The abundance of miR-338-3p in tumor tissues (n=44) and normal tissues (n=44) was examined by qRT-PCR. (G) The negative

correlation between miR-338-3p expression and circ_DLG1 expression was analyzed by Spearman's correlation analysis. (H) MAP3K9 was predicted as a target of miR-338-3p by starBase. (I and J) The interaction between miR-338-3p and MAP3K9 was verified by dual-luciferase reporter assay. (K and L) The expression of miR-338-3p in TE-8 and KYSE450 cells transfected with miR-338-3p and anti-miR-338-3p was detected by qRT-PCR. (M and N) The expression of MAP3K9 in TE-8 and KYSE450 cells transfected with miR-338-3p and anti-miR-338-3p was detected by qRT-PCR and western blot. (O) The negative correlation between miR-338-3p expression and MAP3K9 expression in ESCC tissues was analyzed by Spearman's correlation analysis. *P < 0.05.

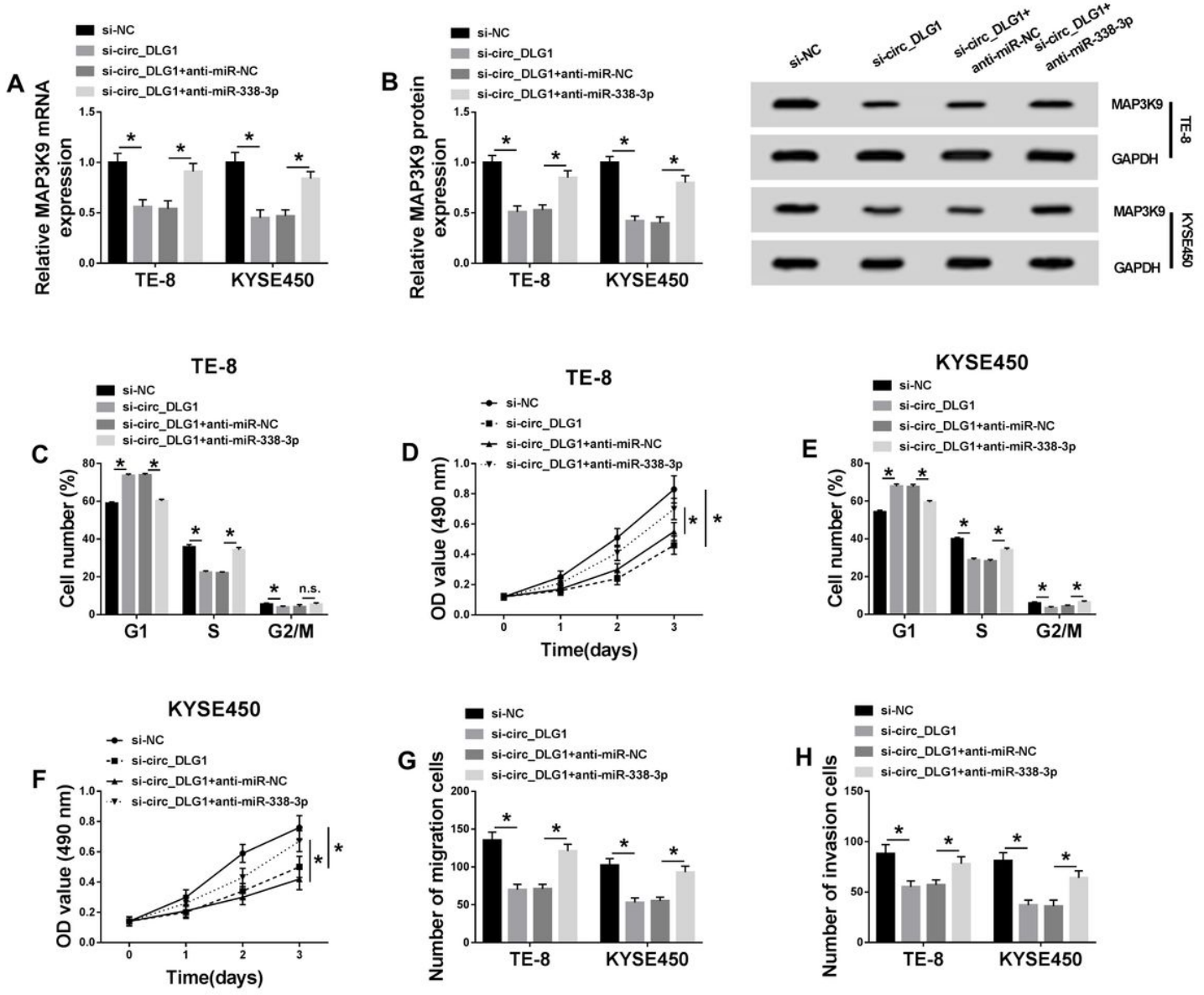

Figure 7

MiR-338-3p downregulation promoted cell cycle, proliferation, migration and invasion blocked by circ_DLG1 knockdown. TE-8 and KYSE450 cells were transfected with si-circ_DLG1, si-NC, si-circ_DLG1+anti-miR-338-3p or si-circ_DLG1+anti-miR-NC. (A and B) The expression of MAP3K9 in these

cells was detected by qRT-PCR and western blot. (C and D) Cell cycle and proliferation in TE-8 cells were assessed by flow cytometry assay and MTT assay, respectively. (E and F) Cell cycle and proliferation in KYSE450 cells were assessed by flow cytometry assay and MTT assay, respectively. (G and H) Cell migration and invasion were evaluated by transwell assay. *P < 0.05.

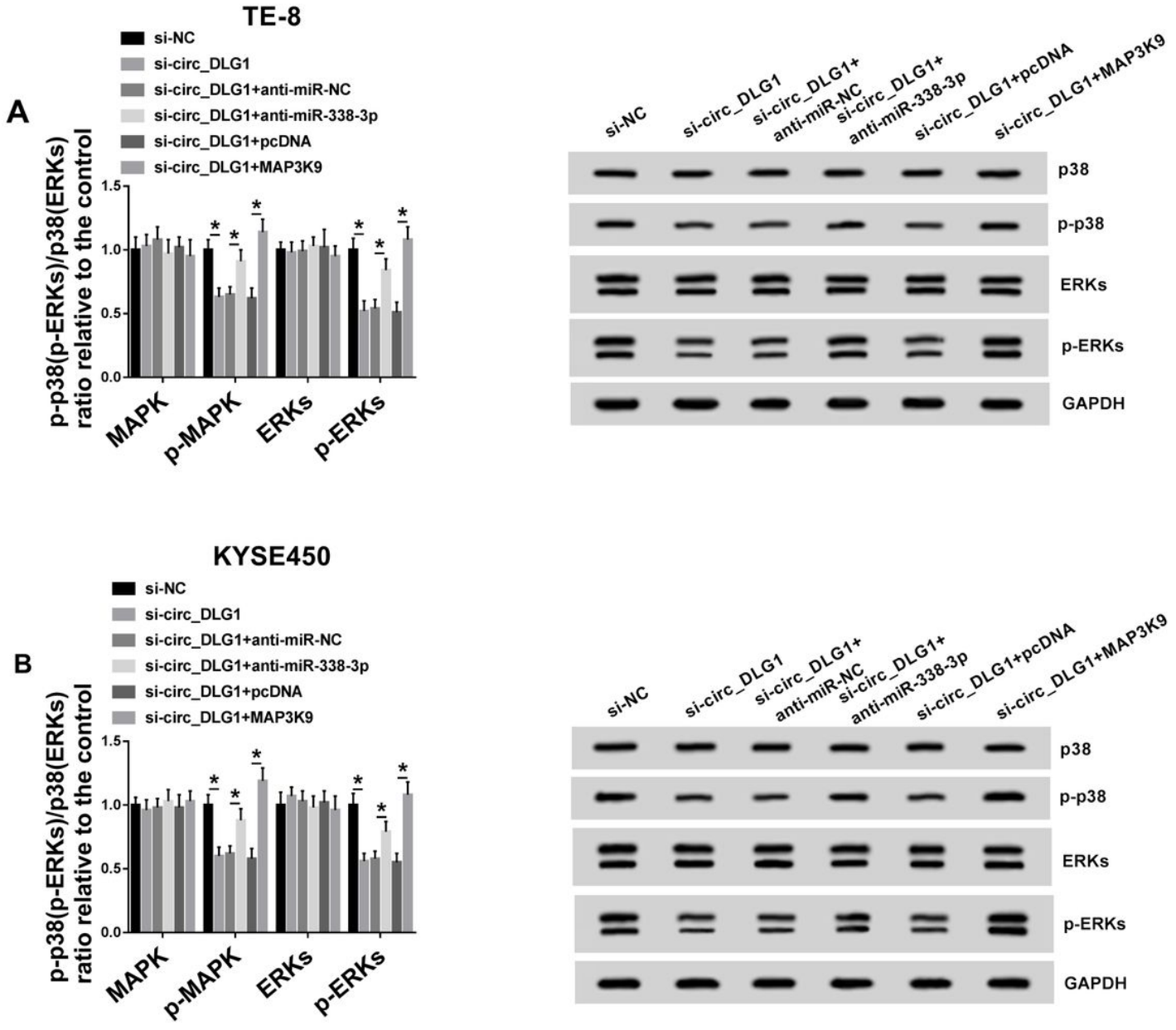

Figure 8

Circ_DLG1 knockdown functioned by inactivating MAPK/ERK pathway. (A and B) The expression of p-p38 and p-ERK was investigated in TE-8 and KYSE450 cells with the transfection of si-circ_DLG1, si-circ_DLG1+anti-miR-338-3p or si-circ_DLG1+MAP3K9, and si-NC, si-circ_DLG1+anti-miR-NC or si-circ_DLG1+pcDNA acted as the separated control. *P < 0.05.

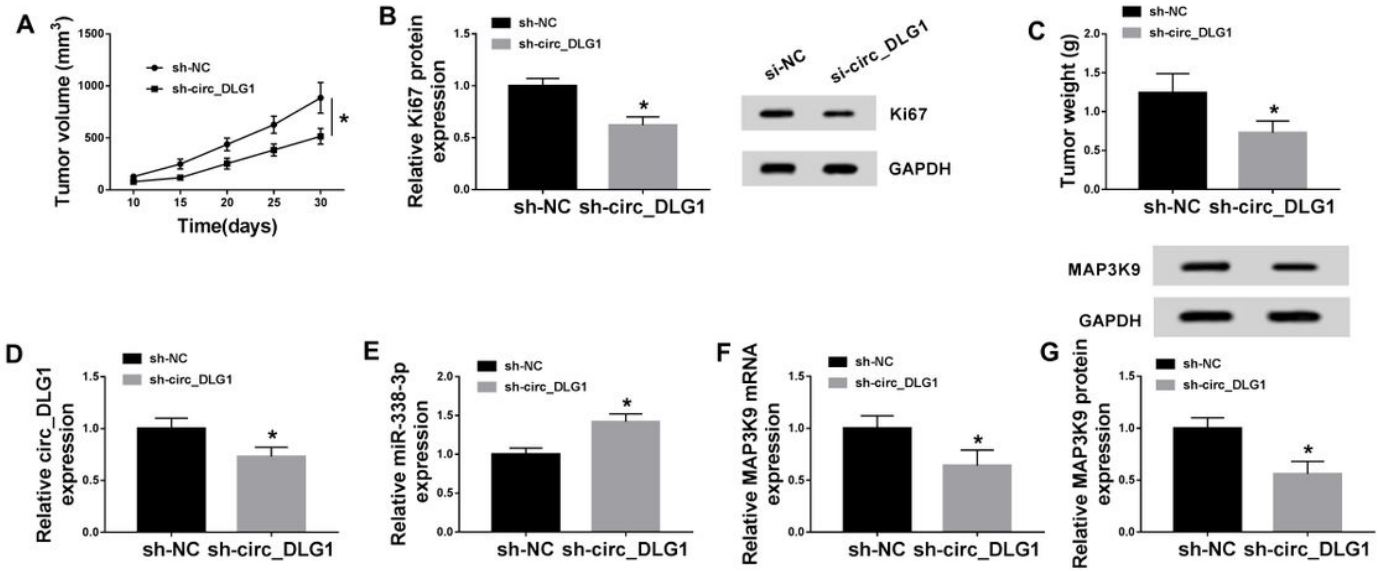

Figure 9

Circ_DLG1 knockdown lessened tumor growth in vivo by downregulating MAP3K9 and upregulating miR-338-3p. (A) Tumor volume was recorded every 5 days. (B) The identification of excised tumor tissues was performed by detecting the expression of Ki67 using western blot. (C) Tumor weight was obtained from the excised tumors. (D and E) The expression of circ_DLG1 and miR-338-3p in tumors was detected by qRT-PCR. (F and G) The expression of MAP3K9 was measured by qRT-PCR and western blot. *P < 0.05.